A Feature-Based Probabilistic Image Segmentation

Hewayda M. Lotfy[1] Adel S. Elmaghraby[1] Mehmed M. Kantardzic[1] Jafar Hadizadeh[2]
University of Louisville
Louisville, KY 40292, USA.
{hmlotf01, adel, mmkant01, hadizadeh} @louisville.edu

Abstract - **Image segmentation can be viewed as a clustering problem in which small image patches are grouped together based on their color and texture features. In this paper, we present a Probabilistic Segmentation Framework (PSF) for segmentation of rock images. Our proposed framework consists of a combination of probabilistic clustering and edge detection technique. The clustering cost function is based on a Maximum-likelihood (ML) estimator. After clustering the pixel-patches based on their features, we approach the improved image segmentation process in two additional steps. First, we map the resulted clusters into the image domain to form subimages. Second, using edge detection on each subimage, we refine and smooth the subimages to finalize the resultant segments. A qualitative comparison of the PSF methodology with alternative techniques using rock images is presented. We demonstrated that the PSF provides the highest quality segmentation amongst the compared techniques.**

I. INTRODUCTION

Object recognition and image analysis depends on image segmentation as a starting point, partitioning segments based on the properties of the individual regions. Segmentation of rock images is crucial for the mining industry, geological sciences, and in space science where rock information is received from digital images sent from space rovers or drilling equipment for rock minerals identification [1]. Experimental rock textures are relatively new in the field of geology and it is used to investigate the effect of fragmentation on minerals, for example during earthquakes. The textural information has been mainly acquired via non-digital methods such as manual or semi-automatic region counting from printed images [2]. These methods, are time consuming, and are heavily dependent on the interpreter's experience. In order to overcome these problems, we have started our collaborative research effort to combine geology experience with computational methods. The result of our collaboration is a set of computerized and efficient segmentation techniques. These techniques are best suited for rock texture analysis. In our earliest effort, we presented an edge detection technique to segment and separate minerals from their background [3]. We selectively use digital filters to reduce the noise prior to edge detection. Following the edge detection, morphological operations are applied including dilation, and filling on the compliment of the image gradient. Malik et. Al. [4] presented their work on gray natural images include rocks that almost have no noise and they introduced a gating operator based on the textured-ness of the neighborhood at a pixel. In their work they presented a localized measure of how two neighboring pixels belong to the same region. Also, they used the spectral graph theoretic framework of normalized cuts to find partitions of the image into regions of coherent texture and brightness. Anderson et. Al. in their work [5] applied Edge-flow and surface density estimation to employ image segmentation for rocks detection. The texture features are the result of using Gabor wavelet decomposition which applies filters at different scales and orientations. The texture feature vectors are then used to cluster the rocks into groups of similar texture using k-means. The author K.B. Eom in [6] represents a texture model as an output of a 2D finite filter with simple input process. The maximum - likelihood (ML) estimators of the model are used as texture features. The texture features are classified with a neural network for supervised segmentation, and clustered by the fuzzy C-mean algorithm. Results are shown on natural and synthetic images. Each of the approaches in [4], [5], and [6] did not handle images with rocks having noise inherited by the experimental settings.

In our work, we are developing a probabilistic framework PSF that segment the rock images efficiently with the presence of noise. The rock images are acquired under experimental and controlled setting. Under these settings, a process of rotary shearing is applied to the rock and magnification degrees ranges from 250x to 1000x are implemented. The shearing process adds sub-micron particles especially when images are acquired in areas where more intense shearing has occurred. This resulted in noise via pixel-scale diffusion of gray levels in addition to the loss of resolution at higher magnifications. These characteristics impose a challenge on the segmentation of the images. Our work is an extension of the contribution introduced in [7].

The PSF methodology enhances images using rank filters. Median filter [8] removes the outliers and preserves more the higher frequencies. In a median filter, a window slides across the data and the median value of the samples inside the window is chosen to be the output of the filter. This nonlinear filter, compared to linear ones, shows certain advantages: edge preservation, smoothing of signals, and efficient noise attenuation with robustness against impulsive-type noise. This is an advantage for rock images because of the random spread of minerals particles perform as outliers and at the same time high frequencies are needed for further image analysis. We have to mention that the median filter may attenuate fine details, sharp corners and thin lines. Despite of the fact that this implies data loss, the

1 Department of Computer Engineering& Computer Science
2 Department of Geography and Geosciences

probabilistic nature of the framework combined with edge detection succeeds to protect many of this information in the form of meaningful and edge preserved segments. The result of rock segmentation is used by a geologist to extract information regarding the mineral particle size distribution changes. In addition, properties such mineral particle size, and mineral shape may be acquired for understanding the mechanics of brittle fragmentation under different conditions. The PSF has two phases. The first phase begins with decomposing the image into subimages and each subimage corresponds to one cluster. Clusters are obtained by the application of probabilistic clustering. We view the image by pixel patches with six different features based on color and texture. The features are used to cluster the patches into subimages. A subimage could consist of several regions and since clustering is performed in the feature space, patches correspond to all image regions that are coherent in the features. The second phase refines the subimages using edge detection and morphological operations.

II. THE PSF METHODOLOGY

The rock images are backscattered Scanning Electron Microscope (SEM) images of simulated granite gouge (gouge is the term used for pulverized rock material found along geologic faults). The gouge samples were deformed in a rotary frictional sliding (shearing) of total displacement ranging from 3mm to 409mm (see [9] for detailed description of materials, methods, and conditions of the experiments). Loss of resolution at higher magnifications results in image noise via pixel-scale diffusion of gray levels. The same effect is also produced due to presence of sub-micron particles in areas of the sample where more intense shearing has occurred. The granite gouge is a loose aggregate of minerals Quartz, K-Feldspar, which they could be distinguished by their different tones of gray on backscattered SEM images. The K-Feldspar is the white particles while the quartz is the gray particles.

A. Image Pre-Processing

The images are converted from RGB into CIE-Lab color space. The Lab color model has three independent components. The L component is the brightness (also called luminosity) and extends from 0 (black) to 100 (white). The a and b are the color components and each of three components can be manipulated separately. The image is enhanced by first applying contrast adjustment and then applying median filter on the L component. The parameters to determine the size of the filter are the magnification and the displacement value. An increase in the rock magnification, displacement, or both implies an increase in the size of the filter which ranges from 11 to 17. For example, an image with 250x magnification and 3mm displacement we apply a filter of size 11 and for an image with 1000x and 409mm we apply a filter of size 17. In order to reduce the amount of data presented to the clustering algorithm while preserving the information needed for image analyzing. Each of the L, a, and b components are uniformly partitioned into *BxB* patches. In our case *B* is 4. If each component is of size *MxN* and divided by square patches of size B then the resulted number of patches is n=M_BxN_B, where $M_B = \lceil M/B \rceil$ and $N_B = \lceil N/B \rceil$. Figure 1 shows the results of an application of a median filter of size 13 on an image of magnification 250x and of displacement 3mm. The median filter is applied to the L-component and shown in figure 1-b). The gray levels representing a mineral particle became closer and much of the noise was removed.

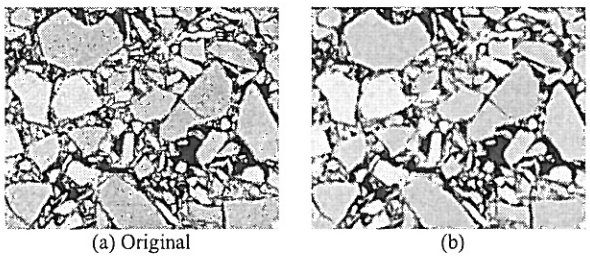

(a) Original (b)

Figure 1: Application of median filter of size 13 on L-component of an image has 250x and 3mm displacement

B. Feature Extraction

Many of feature extraction techniques have been based on the combination of color and texture features [10]. The shape features provide better results for isolated shapes. We extract for each patch, six features three of which are color features and three are texture features. The color features are extracted from the color layout technique [11]. In color layout, the image is represented by its local characteristics. The average color is calculated for each patch in each component (*L*, *a*, and *b*) resulting in a three component average vector for each patch. The three color features of a patch *i* are named $f_{i,1}$, $f_{i,2}$, and $f_{i,3}$, i=1,...,n . The texture features are extracted from the 2D wavelet transform which is a multi-scale image representation where the image can be represented at different levels of detail. The idea of wavelet is to use the features of the wavelet coefficients at the coarse scale levels. The 2D-filtering decomposes an image into signals; three of them are detail signals which are directionally sensitive: *LH, HL, and HH* emphasize the horizontal, vertical, diagonal features respectively. The energy in the high bands, where texture lies, is the square root of the second order moment of wavelet coefficients. To obtain these moments, a one-level Daubechies wavelet transform is applied to each of the patches. The texture features of a patch *i* are named $f_{i,4}$, $f_{i,5}$, and $f_{i,6}$, i=1,...,n. The feature $f_{i,4}$ is computed from the coefficients of the *LH* band $\{a_{k,l}, a_{k,l+1}, a_{k+1,l}, a_{k+1,l+1}\}$ as in equation 1.

$$f_{i,4} = \left(\frac{1}{4} \sum_{i=0}^{1} \sum_{j=0}^{1} a_{k+i,l+j}^2 \right)^{\frac{1}{2}} \quad (1)$$

Similarly, the features f_5, and f_6 are computed but f_5 is computed from the HL band while f_6 is computed from the

HH band. The process of feature extraction will bring out a feature vector F of size nx6, the features of patch i is $F_i = (f_{i,1}, \ldots, f_{i,6})$ where $i=1, \ldots, n$. The vector F is normalized by normalizing each of the six features by its mean and standard deviation. Normalization gives each feature an equal contribution.

C. *The PSF Segmentation*

In PSF first phase, we use the Expectation Maximization (EM) algorithm as the probabilistic clustering approach [12] [13] of the framework. We have chosen EM because it is known for its robustness to noisy data. EM can be used as ML estimator. It is convenient to recast the problem in the equivalent form of minimizing the negative log likelihood of the data set. Since EM is an iterative algorithm we set the maximum iteration to 150 iterations. We found that the average of the minimum negative Likelihood for the image dataset is reached with $k=4$ at iteration 105. In PSF second phase, we apply edge detection and morphological operations on the Quartz and K-Feldspar subimages obtained from clustering. The framework was implemented using Matlab 6.5 and the EM main functions are obtained from the Netlab Toolbox [14].

To determine number of clusters k we used the Adjusted Rand Index (ARI). ARI [15] is a measure of the agreement between two detected partitions since we assume each patch in the features vector is assigned to only one class. The ARI can measure the difference of two partitions even when the number of clusters is different, and its value lies between 0 (no agreement) and 1 (total agreement). For the comparison between two partitions, two contingency matrices is computed that define which cluster each entity has been assigned to. Given a set of n objects $S=\{O_1, \ldots, O_n\}$, suppose that $P=\{p_1, \ldots, p_R\}$ and $Q=\{q_1, \ldots, q_C\}$ represent two different partitions of the objects in S such that

$$\bigcup_{i=1}^{R} p_i = S = \bigcup_{j=1}^{C} q_j \qquad (2)$$

, and

$$p_i \cap p_{i'} = \phi = q_j \cap q_{j'}, 1 \le i \ne i' \le R, 1 \le j \ne j' \le C \qquad (3)$$

We calculate the ARI for a number of repetitions r (maximum 8) of running EM and each repetition automatically calculates a number of clusters k (see [7]) and a corresponding partition. For each pair of repetition x and y, where $x, y = 1, \ldots, r$, the ARI (P_x, P_y) is computed where P_x *and* P_y denotes partitions corresponding to repetition x and y. Then for all $x=1, \ldots r$ the meanARI(P_x)= mean (ARI (P_x, P_y)) for all $y=1, \ldots r$ is evaluated. The maximum *meanARI* points out to the partition that has the maximum agreement with the all other partitions. The ARI implementation shows that the best number of clusters describing our rock images is k=4. Hence, when ordered from the highest gray level to the lowest, the clusters represent the K-Feldspar, the Quartz, the grinded materials (gray background) and finally the black pores. We use random initialization of centers using the number of feature vectors then the initial centers are chosen at intervals starting from the beginning of the feature vector and the interval is defined to be the quadrant of the number of features. We have trained the model using different initialization to ensure obtaining good models.

K-Leveled Image: The block-cluster membership is visualized by assigning the cluster centroid to every patch that belongs to the corresponding cluster constructing a new image array. The patches positions of the original image are pre-stored to assist in assigning the centroids to its cluster patches in the correct position and the result of this assignment is called a K-Leveled image.

Edge Detection and Morphology: This is the second phase of the framework and used for segmentation refinement and as a tool to obtain more linear edges. We derive four subimages the same way as we did with the K-Leveled image but restricting the extraction to one specified class instead of all classes. On Quartz and K-feldspar particles subimages we apply an erosion operation using the disk structuring element with radius 1 for opening the closed thin lines representing minerals fine particles surrounding other minerals in the rock. Second, an application of canny edge detection is followed by filling the resulted gradient. Minerals particles at the image borders or those less than 50 pixels are discarded because it is incomplete or insignificant respectively. This phase of PSF is extremely useful especially the use of morphological operations with quartz subimages. Usually, the binary mask of quartz (see figure 2-d) have more thin lines than the feldspar since quartz has more similar intensity values to the gray background.

III. EXPERIMENTAL RESULTS

This section presents results of applying PSF approach on images that have rocks that went under different conditions of shearing and magnification. The shearing is represented by the displacement value where 3mm is the least displacement applied on the rock resulting in minor fragmentation while 409 mm is the largest displacement resulting in major fragmentation. The rocks in figure 2-a) have 250x magnification and 3mm displacement this mean it has the less noise. Figure 2-b) shows the K-Leveled image where $k=4$, in which the minerals particles are distinguished and separated from each other. The particles of K-feldspar and Quartz are shown in figure 2-c) and figure 2-d) respectively. In figure 3-a) the rock magnification is 500x and the displacement is 3mm. Figure 3-b) display the K-Leveled image and the K-feldspar and quartz particles are in the subimages shown in figure 3-c) and figure 3-d) respectively.

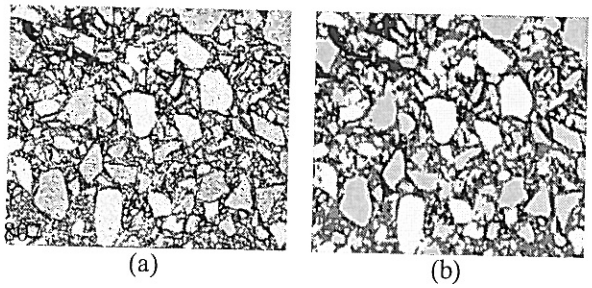

(a) (b)

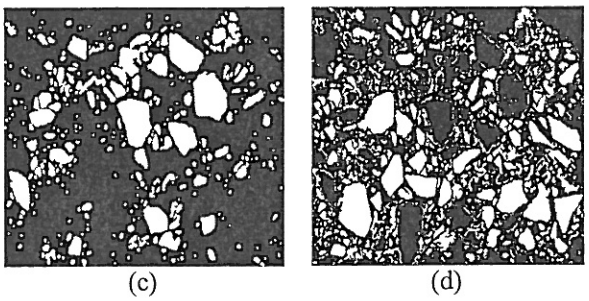

(c) (d)

Figure 2: (a) Original image, (b) K-Leveled image, (c) The K-Feldspar particles (d) The Quartz particles

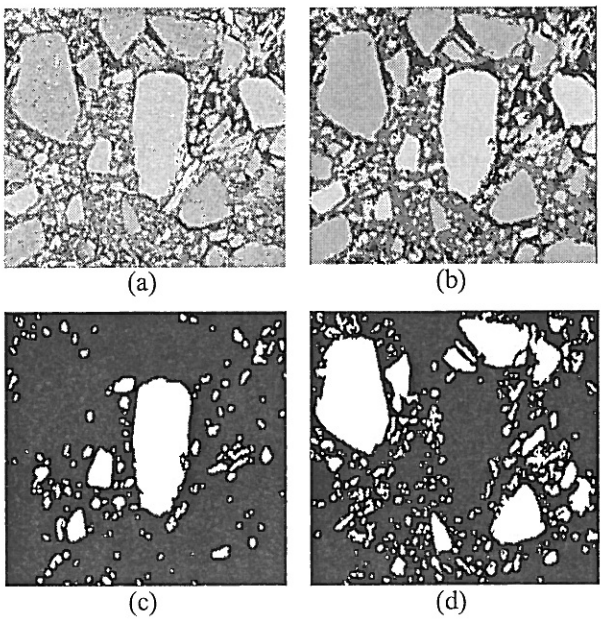

(a) (b)

(c) (d)

Figure 3: (a) Original, (b) K-Leveled image (c) PSF K-Feldspar particles and (d) PSF Quartz particles

The Image in figure 4 has more noise due to 65mm displacement and 1000x magnification. The EM clustering of this image tolerated this noise and the PSF result is shown in figure 4-b).

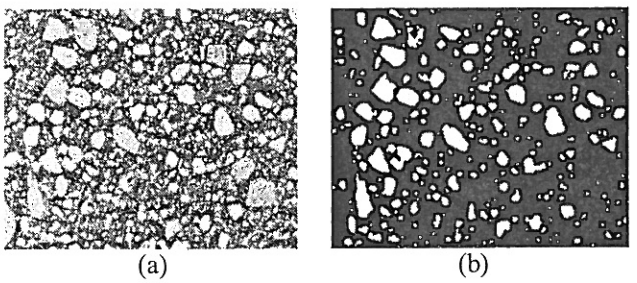

(a) (b)

Figure 4: (a) Original, and (b) PSF K-Feldspar particles

Figure 5-a), presents the negative minimum likelihood value is monotonically decreasing with the increase of iteration until it stops decreasing and that is when EM converges. Figure 5-b) shows the minimum negative likelihood Value reached for each image in the image dataset.

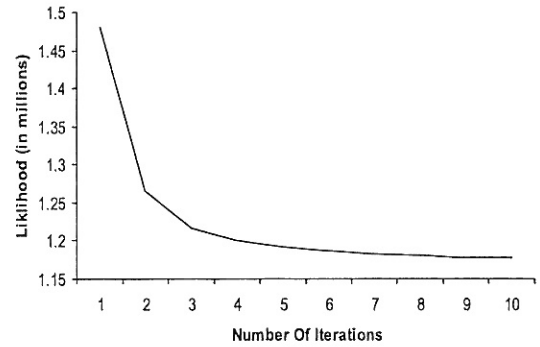

(a)

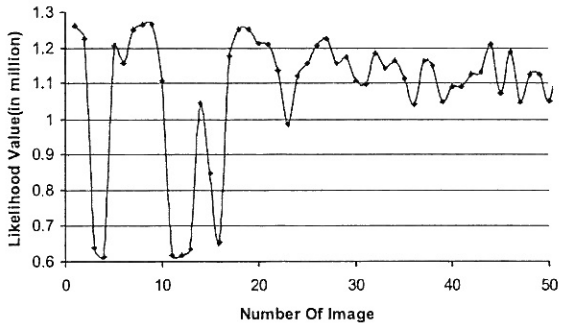

(b)

Figure 5: EM Minimum Likelihood Results

IV. EVALUATION OF RESULTS

The experiments involved room temperature shearing of the simulated gouge by frictional sliding displacement. A set of 51 images studied here underwent from 3mm to 409mm of total rotary displacement. The images [9] are RGBs of average size 980x1400 and were taken at SEM magnifications 250x, 500x, or 1000x of the original rock. In this section we evaluate PSF by comparing the results of with other clustering models such as Kmeans [5], and FCM (Fuzzy C-Mean) [6] where number of clusters is $k=4$. The criteria considered for comparison are the perceptional quality of segmentation and clustering execution time. The image preprocessing steps, feature extraction, and K-Leveled image construction, as discussed in section II, is the same for Kmeans and FCM. In figure 6, the PSF, Kmeans and FCM K-Leveled images are presented. The rocks in the image in figure 6-a) has been exposed to maximum magnification 1000x and maximum displacement 409mm and this makes it hard to segment. An expert estimated that the results of PSF in figures 6 and 7 are better than that of Kmeans and FCM and the segmentation resulted from FCM is better than that of Kmeans. The criterion determined by the expert is that the selected technique is the technique that provides the more separated and the less eroded or missed minerals particles.

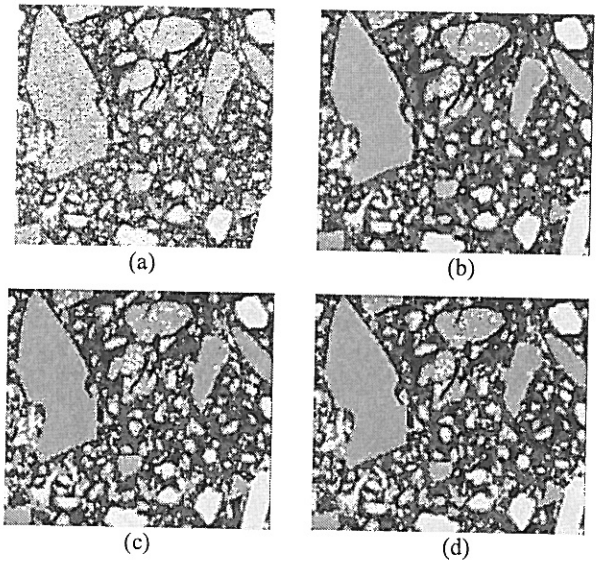

Figure 6: (a) Original, (b) EM K-Leveled, (c) Kmeans K-Leveled, and (d) FCM K-Leveled

Figure 7 depicts (in pairs) the quartz particles segmentation before and after refinements of the K-Leveled images in figure 6 after applying the second phase of PSF. Figures 7-a) and 7-b) show the binary mask of PSF K-Leveled image before and after second phase respectively. Figures 7-c) and 7–d) are the binary mask of Kmeans K-Leveled image before and after PSF second phase. Finally, figures 7-e) and 7-f) are the binaries of FCM before and after the PSF second phase. In figure 7-a) the edges of the minerals are thinner, linear and separated than in of figures 7-c) and 7-e). This resulted in better final segmentation in figure 7-b) and meaningful particles to the geology expert and hence considered figure 7-b) is the highest quality obtained. Figures 7-c) and 7–e) reveals that their particles are more connected to other particles and to the borders. This resulted in the lost of the largest particle when the second phase was applied as presented in figures 7-d) and 7-f).

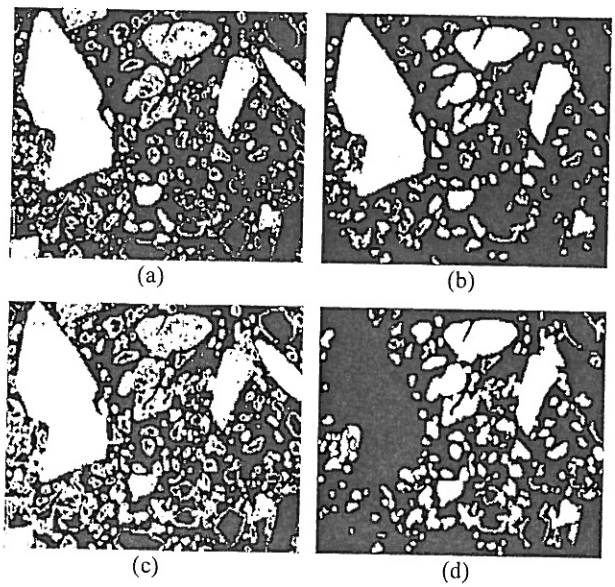

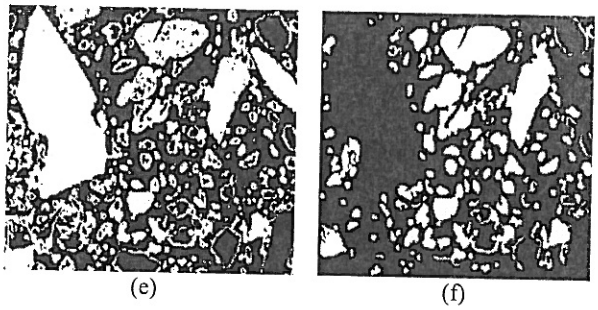

Figure 7: (a) and (b) PSF-Quartz, (c) and (d) Kmeans & second Phase-Quartz, and (e) and (f) FCM& second phase-Quartz

Figure 8 describes the results of another comparison between PSF, Kmeans, and FCM using an image of 500x with displacement 509mm. The resulted binaries in figure 8-c) and 8–d) have lost whole particles while in figure 8-b) the segmentation has the highest quality, the minerals particles are more linear and more separated from other edges.

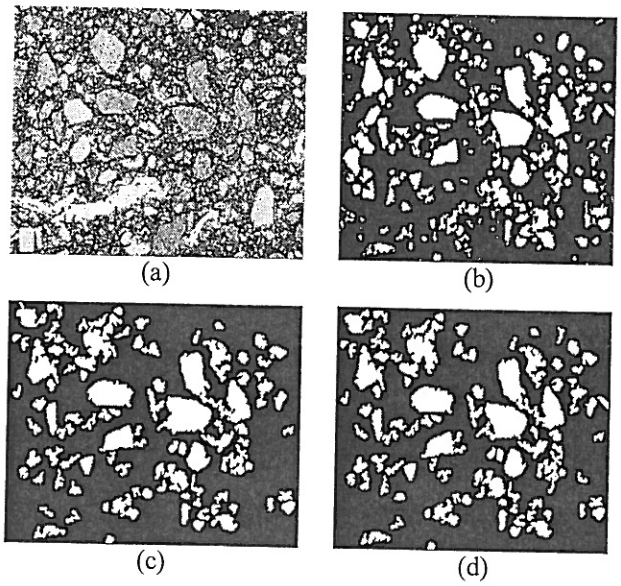

Figure 8: (a) Original, (b) PSF-Quartz, (c) Kmeans & second Phase - Quartz), and (d) FCM & second phase-Quartz

For the perceptual quality, a geologist conquered that PSF segmentation is better than FCM and Kmeans with the second phase. Using visual inspection we were able to quantify the performance of the three alternative techniques applied to the test images. The geologist was given 153 images in which for each image in the image dataset there is three binary images, one resulted from PSF, and the other two resulted from Kmeans and FCM after second phase. The geologist rated for the PSF methodology 46 images out of 51 images as the highest quality segmentations obtained to be used for further interpretation and rated for the segmentation of FCM combined with PSF second phase 26 images of 51 images as high quality. Finally, the geologist rated for the segmentation of Kmeans combined with PSF

second phase 1 image out of 51 images as high quality. In table 1, the results of the comparison of the application of the three techniques on the image dataset are reported, 90% of the images have high quality segmentation using PSF while 51% of them have high quality segmentation with FCM, and almost 0% of the images have high quality segmentation with Kmeans. Another consideration for evaluation is the average execution time for the clustering techniques shown in table 1. For EM, the average execution time is slower than Kmeans and FCM. The reason for this is because EM spends more time for the probabilities and covariance matrices calculations but this was substituted in the quality of the segmentation obtained as stated in table 1.

TABLE I

Percentage of Quality of segmentation and Average execution time per image of PSF, FCM, and Kmeans

Method	High Quality Segment. Percent.	Average Execution Time
Kmeans+2nd Phase	0.02%	64.924 sec
FCM+2nd Phase	50.9%	69.408 sec
PSF	90.1%	80.729 sec

V. CONCLUSIONS AND FUTURE WORK

In this paper, we have presented a new framework PSF that seems well adapted to rock image segmentation. PSF has two phases, the clustering phase, and a refinement phase. In the first phase, EM clusters the image using the ML estimation. EM is robust to the image noise and provides better subimages. In the second phase, the edge detection and morphological operations provide linear and representative edges similar to the original and hence the resulted segments are more meaningful. The second phase can be considered as a substitute to the time consuming post-processing especially for the quartz subimages. We compared the PSF methodology with the fuzzy C-mean and Kmeans and we found that the PSF outperformed Kmeans and FCM and provided the highest quality obtained for segmentation. The PSF gives a promising segmentation result. Our future work will provide an integrated framework for PSF segmentation and region content–based retrieval of rock images.

VI. ACKNOWLEDGMENT

This research was partially supported by the U.S. National Science Foundation grant EAR0229654 to Hadizadeh.

VII. REFERENCES

[1] Fox, J, R. Castano, and R. C. Anderson, "Onboard Autonomous Rock Shape Analysis for Mars Rovers", IEEE Aerospace, 2002.

[2] Herwegh, M., "A New Technique to Automatically Quantify Microstructures Of Fine–Grained Carbonate Mylonites: Two Steps Etching Combined With SEM Imaging and Image Analysis", Journal Of Structural Geology 22, pp. 391-400, 2000.

[3] Lotfy H., Hadizadeh J., Elmaghraby A., "Segmentation Techniques for Image Analysis of Fragmental Rock Textures.", Proc. Intl. Conf. IASSE-2003, pp 93-96.

[4] Jitendra Malik, Serge Belongie, Jianbo Shi, and Thomas Leung, "Contour and Texture Analysis for Image Segmentation", Int. Jrnl of Comp. Vision, 2000.

[5] R. C. Anderson, R. Castano, T. Stough, V. Gor, and E. Mjolsness, "Using Scaled Visual Texture for Autonomous Rock Clustering", Abstract 2103, Lunar and Planetary Science Conference 2001

[6] K. B. Eom, "Segmentation of monochrome and color textures using moving average modeling approach", *Image and Vision Computing Journal,* vol. 17, no. 3, pp. 231-242, 1999.

[7] H.M. Lotfy, A. S. Elmaghraby, M. M. Kantardzic, J. Hadizadeh, "Expectation-maximization framework for Rock textures segmentation", to appear 2004.

[8] I. Pitas and A.N. Venetsanopoulos, *Nonlinear Digital Filters:Principles and Applications*, Kluwer Academic Publisher, 1990.

[9] Beeler N. M. and T. E. Tullis, "Frictional Behavior Of Large Displacement Experimental Faults", Journal Of Geophysics Research, Vol. 101, 1996.

[10] Selim Aksoy, et. al, "Probabilistic vs. Geometric Similarity Measures for Image Retrieval", in Proc. of IEEE Int. Conf. on CVPR, V2, 2000.

[11] Yong Rui, , et Al., "Image Retrieval: Past, Present, and Future", Intl. Sym. on Multimedia Inf. Proc. 1997.

[12] Geoffrey Mclachan, David Peel, Finite Mixture Models, Wiley Series in Probabilities and Statistics, 2001.

[13] Chad Carson, et. al, "Blobworld: Image Segmentation Using Expectation-Maximization and Its Application to Image Querying.", IEEE Trans. on Pattern Anal. and Machine Intelligence, 24(8), pp. 1026-1038, 2002.

[14] I.T. Nabney, NETLAB: Algorithms for Pattern Recognition, Springer, 2002.

[15] K.Y. Yeung and W.L. Ruzzo, "Principal component analysis for clustering gene expression data.", Bioinformatics, 17(9):763-774, 2001.